Interannual Changes of Tropical Cyclone Prevailing Tracks in the Western North Pacific

Haikun Zhao, Liguang Wu, and Weican Zhou

Key Laboratory of Meteorological Disaster of Ministry of Education
Nanjing University of Information Science and Technology

April 10, 2010

Submitted to 29th Conference on Hurricanes and Tropical Meteorology

Corresponding author address: Haikun Zhao
Key Laboratory of Meteorological Disaster of Ministry of Education
Nanjing University of Information Science and Technology, Nanjing 210044
E-mail:zhk2004y@nuist.edu.cn

* The manuscript has been accepted by Advances in Atmospheric Sciences, doi: 10.1007/s00376-010-9161-9. Note that the title of manuscript published in AAS had been changed to "Assessing the Influence of ENSO on Tropical Cyclone Prevailing Tracks in the Western North Pacific"

1. Introduction

The interannual variations of tropical cyclone (TC) activity in the western North Pacific (WNP), which are closely related to El Niño-Southern Oscillation (ENSO), have been extensively discussed in the literature (Chan 1985; Dong 1988; Lander 1994; Chen et al. 1998; Wang and Chan 2002; Chia and Ropelewski 2002; Chu 2004; Camargo and Sobel 2005; Camargo et al. 2007). Attention in previous researches was primarily paid to the TC formation with a general consensus that ENSO affects the location of TC formation in the WNP (Li 1985, 1986; Wu and Lau 1992; Chan 2000; Wang and Chan 2002). Wang and Chan (2002) found the enhanced TC formation in the southeast quadrant of the WNP basin during strong El Niño years, suggesting a southeastward shift in the mean TC formation location during El Niño years compared to La Niña years. Previous studies investigated the ENSO influence on TC tracks, mainly in terms of the associated TC landfalls (Saunders et al. 2000; Wang and Chan 2002; Liu and Chan 2003; Wu et al. 2004; Fudeyasu et al. 2006; Camargo et al. 2007). Some of these studies argued that the impact of ENSO on TC tracks was relatively small compared to Antarctic oscillations (Yoo et al. 2004; Ho et al 2005).

On the other hand, in association with ENSO, Chan (1994) and Camargo et al. (2007) identified large variability in TC tracks. Wang and Chan (2002) found that during the fall of strong warm years, the number of TCs that recurve northward increased significantly. Saunders et al. (2000) argued that ENSO had a remarkable impact on the landfall pattern of TCs in Vietnam and the Philippines. Wu et al. (2004) also showed the ENSO impact on TC landfall activity in the WNP, East Asia, and Southeast Asia. Similarly, Fudeyasu et al. (2006) examined the ENSO influence on

TC landfall characteristics during the peak TC season in the Korean Peninsula and Japan, China, and the Indochinese Peninsula. Ho et al. (2005) argued that Antarctic oscillations have more significant influence on large-scale circulations and thus TC track patterns especially in the East China Sea and East Asia than the ENSO. To date, the ENSO influence on TC prevailing tracks in the WNP basin is still not well understood. In particular, how changes in large-scale atmospheric circulation and TC formation locations affect TC prevailing tracks is not quantitatively addressed. One of the possible reasons is lack of an effective diagnostic tool for quantitatively identifying the contributions of changes in large-scale atmospheric circulation and TC formation locations.

In recent years, the influence of global warming on TC intensity has received extensive attention (Knutson and Tuelya 2004; Emanuel 2005; Webster et al. 2005; Trenberth 2005; Hoyos et al. 2006; Kossin et al. 2007; Wu and Wang 2008; Wu et al. 2008). Studies also documented interdecadal changes in typhoon tracks (Ho et al. 2004; Wu et al. 2005; Tu et al. 2009). Some studies found that the overall TC-associated precipitation in China decreased over the past decades (Ren et al. 2006), but with increasing floods in the Yangtze River Valley (Gong and Ho 2002). A few studies have focused on possible changes in TC tracks under the background of global warming. With large-scale environmental flows from global warming experiments, Wu and Wang (2004) proposed a trajectory model to assess the possible impacts of global warming on TC prevailing tracks in the WNP. Emanuel et al. (2006) incorporated a similar trajectory model into their statistical deterministic system that

includes separate models for predicting TC formation, motion and intensification. These studies provide a useful way for understanding the interannual variations of TC prevailing tracks.

In this study, our objective is twofold. First, the capability of the trajectory model is evaluated on the interannual time scale. Second, the roles of the interannual changes of formation locations and large-scale environmental flows in TC prevailing tracks are quantitatively examined by statistically generating a large sample of formation positions and using the trajectory model. The rest of the paper is organized as follows. The data and selection of El Niño and La Niña years are described in section 2. In section 3, the observed changes in the prevailing tracks in the WNP basin are discussed. The statistical approach for generating TC formation locations and TC trajectory model are introduced in section 4. The influences of changes in the formation location and environmental flow on TC prevailing tracks during El Niño and La Niña years are investigated in section 5, followed by a summary in section 6.

2. TC translation vectors and selection of El Niño and La Niña years

On average the WNP basin experiences 26 TCs each year, accounting for about 33% of the global TCs. The TC data in the WNP basin are the best track dataset from Joint Typhoon Warning Center (JTWC), including positions and intensities of tropical storms and typhoons at six-hour intervals. Our analysis period ranges from 1950 to 2007 in this study. Although some TCs over the WNP basin might be missed in the JTWC best track data before the satellite era and TC intensity estimates prior to 1970 include uncertainty, we find that their influences on our analysis results are little

because the difference of the prevailing track between El Niño and La Niña years is essentially the same when we use the data from 1970 to 2007 and only TC track data are used. Note that although TCs can occur all the year around in WNP basin, we only use the data for the peak TC season, namely from July to September, because the TC activity is so frequent in the peak season that the climatological mean winds can represent the large-scale steering flows (Wu and Wang 2004). The climatological wind data are from the NCEP Re-analysis monthly fields with a uniform latitude-longitude 2.5° resolution grid. By assuming that TCs are short lived and transient phenomena compared to climate change (Wu and Wang 2004), the mean large-scale steering flows for the El Niño and La Niña years are calculated as the mean environmental flows averaged between 850 and 300 hPa with mass adjustment.

The mean translation speed and beta drift of TCs are calculated over the TC peak season for El Niño years and La Niña years. Following Wu and Wang (2004), consistent with the resolution of the large-scale steering flows, we represent the WNP basin with 2.5º latitude by 2.5º longitude grid boxes. For each box, a mean translation speed is calculated based on all of the TCs that entered the grid box for El Niño years and La Niña years, respectively. Note that the mean translation vectors and mean beta drift are calculated only for each grid boxes with the sample size exceeding once a year.

The interannual variations of the TC activity in the WNP have been documented in previous studies, which are closely correlated with the Niño-3.4 (5° S–5° N; 170° W–120° W) sea surface temperature anomalies (SSTAs) (Chan 1984;

Lander 1994; Wang and Chan 2002). In this study, the Niño-3.4 SSTAs from the Climate Prediction Center are used to stratify the warm and cool years using the percentile method proposed by Camargo et al. (2007), in which the 25% of warmest and coldest years are selected. As shown in Fig. 1, the years with the SSTA larger (less) than 0.47°C (-0.47°C) are defined as El Niño and La Niña years, respectively. The other years are classified as neutral years. Thus we select 14 El Niño years (1951, 1953, 1957, 1963, 1965, 1969, 1972, 1982, 1987, 1991, 1997, 2002, 2004, and 2006) and 14 La Niña years (1950, 1954, 1955, 1956, 1959, 1964, 1970, 1971, 1973, 1975, 1988, 1998, 1999, and 2007).

The El Niño and La Niña years defined in this study generally agree with those from other methods (Trenberth 1997; Goddard and Dilley 2005). In Wu et al. (2004), the ENSO years were identified with the 5-month running mean SSTAs in the Niño -3.4 region with a SSTA threshold of 0.4°C (-0.4°C) for 6 months or more. Wang and Chan (2002) also used a threshold of 0.4°C (-0.4°C) to classify the ENSO events, but for the Niño-3.4 SSTA in the peak TC season. It should be pointed out that the selected warm and cool years are only slightly different. For example, Wang and Chan (2002) also classified 1994 and 1967 as warm and cool years, respectively.

3. Changes of the prevailing TC tracks on the interannual time scale

Figure 2 shows the differences of the TC translation vectors (Fig. 2a) and large-scale steering flows (Fig. 2b) between El Niño and La Niña years. The changes in the TC translation vectors can be largely accounted for by the differences in the large-scale steering in terms of both of the direction and magnitude. Over the WNP,

the westerly (easterly) anomalies of the large-scale steering agree well with the eastward (westward) anomalies of the TC translation vectors north (south) of 24° N. In the South China Sea, the changes in the TC translation vectors are mostly southeastward and eastward over the northern and southern parts, respectively, also well consistent with the corresponding changes in the large-scale steering.

Previous studies suggested that the mean translation speed is the sum of the climatological mean large-scale steering flow and beta drift (Holland 1983; Wu and Wang 2004). The beta drift in El Niño and La Niña years are derived as the difference between the translation vectors and large-scale steering flows (figure not shown). Although large-scale environmental flows can affect beta drift (Ulrich and Smith 1991; Smith 1991; Williams and Chan 1994; Wang and Li 1995; Li and Wang 1996; Wang et al. 1997, Zhao et al. 2009), the differences of the beta drift between El Niño and La Niña years are found to be very small in this case. For this reason, we do not consider the influence of the beta drift change on TC prevailing tracks in this study.

The prevailing TC tracks are determined based on the frequency of TC occurrence, which is defined on each grid box of 2.5° latitude by 2.5° longitude (Wu and Wang 2004). The frequency indicates how often TCs affect a specific grid box. In this study, as shown in Fig. 3, the climatological prevailing tracks are detected as the grids with high frequency relative to the adjacent grids. In the WNP basin, three climatological prevailing tracks are identified in the peak season (thick arrows in Fig.3) during the period 1951-2007, which are used as a reference for examining track changes during El Niño and La Niña years in this study. First, a westward-moving

track extends from the tropical Pacific to the Philippine Sea and the South China Sea (the westward track or track I). Second, TCs move northwestward from the tropical Pacific to Korea and Japan (the northwestward track or track II), influencing the coastal region of East Asia and the surrounding waters. Third, TCs take the prevailing track recurving northeastward east of 140°E (the recurving track or track III). In addition, the identified prevailing tracks I, II, and III account for 23%, 53%, and 24% of all tracks, respectively, and the large red dots indicate the relatively concentrated positions of tropical cyclone formations.

Although the total numbers of TCs are nearly the same in the peak season for El Niño (181 TCs) and La Niña years (180 TCs), the changes in the frequency of TC occurrence or prevailing tracks can be clearly seen in Fig. 3. While the westward track (track I) slightly shifts northward and reduced TC activity east of 150° E in the La Niña years, TCs taking the northwestward prevailing track, by which TCs affect East Asia, including Taiwan Island, China mainland, Korea and Japan, tend to move more westward in the El Niño years while taking a more northward track in the La Niña years. The enhanced TC activity is also clearly shown in the difference of TC occurrence between the El Niño and La Niña years (Fig. 4). In general, the TC occurrence increases south of 20° N during the El Niño years. Using the Mann-Kendall test (Kundzewicz and Robson. 2000), the statistically significant changes at the 95% level occur mainly in the tropical Pacific east of 130° E. This is consistent with the enhanced TC formation in the southeast quadrant of the basin (Wang and Chan 2002).

4. TC formation and trajectory models

While the impacts of global climate change on TC tracks were investigated with a simple trajectory model in previous studies (Wu and Wang 2004; Emanuel et al. 2008), TC track changes on the interannual timescale received little attention, mainly because of lack of sufficient TC samples. Following Hall and Jewson (2007), a basin-wide stochastic formation simulation model is adopted for El Niño and La Niña years in the WNP basin in this study. Similar approaches have been used by James and Mason (2005) and Emanuel et al. (2006) and Emanuel et al. (2008).

The statistical TC formation model is based on the historical TC formation locations during El Niño and La Niña years (Fig. 5). During the El Niño years, there are three TC formation maxima, which are located in South China Sea, east of the Philippines, and over the area of 10-15° N and 140-150° E (Fig. 5a). As shown in Fig. 5b, the third formation maximum disappears during the La Niña years. One of the reasons may be the expansion of the warm SST in El Niño years (Wang and Chan 2002). Then we construct a two-dimensional (latitude and longitude) probability density function (PDF) from the observed information. The Gaussian kernels include anisotropic variance length scales δ_1 and δ_2, which are referred to as the bandwidths of the formation PDF. The formation PDF at (x,y) takes the form of

$$f(x,y)=\frac{1}{2\pi N\delta_1\delta_2}\sum_{i=1}^{N}\exp[-\frac{(x-x_i)^2}{2\delta_1^2}-\frac{(y-y_i)^2}{2\delta_2^2}], \qquad (1)$$

where N is the numbers of TCs, x_i, y_i are the longitudes and latitudes of historical formation locations, δ_1 and δ_2 are bandwidths in the latitudinal and longitudinal directions. Here we assume that the direction bandwidths are equal in the longitudinal

and latitudinal directions. Formula (1) becomes

$$f(x,y)=\frac{1}{2\pi N\delta^2}\sum_{i=1}^{N}\exp[-\frac{(x-x_i)^2+(y-y_i)^2}{2\delta^2}], \qquad (2)$$

To obtain the optimal bandwidths for El Niño and La Niña years, the bandwidth needs to be determined using the cross-validation method (Fig. 6).

To show the importance of the optimal bandwidth, the kernel PDF with three different bandwidths for the El Niño year simulation is shown in Fig. 7. The PDF is calculated using (2) with the bandwidths of 1.5°, 2.9°, and 5°, respectively. The bandwidth of 1.5° gives under-fitted formation simulation because of too many local maxima, while the bandwidth of 5° shows over-smoothed simulation locations only with one maximum. In this study, we take the bandwidth of 2.9° as the optimal one, which makes the kernel density maximum. For the La Niña years, the optimal bandwidth is set to 3.4°. With the optimal PDFs, TC formation locations (latitude and longitude) can be simulated with a uniform random number generator. A formation location is selected only if it satisfies the observed PDF calculated with (2). This procedure continues until all of the required formation locations are obtained. In this study, ten times as many points as observed formation locations are simulated during El Niño and La Niña years (Fig. 8) and the distribution of the frequency simulation of formation positions agrees well with the observed distribution of formation locations (Fig. 5).

Considering TC motion is mainly determined by climatological mean beta drift and large-scale steering flows. Wu and Wang（2004）showed that the prevailing TC tracks can be simulated using a trajectory model. In this study, all the TCs that are formed over the peak TC season for El Niño and La Niña years are considered to construct the climatological mean translation vectors while the formation positions are

derived from the formation simulation model. Since the climatologic motion vectors at some grids are not available, their translation velocity is taken as the sum of the mean steering flow and the mean beta drift that was computed by averaging the beta drift over all the grids at which the climatological motion vectors are available. The TC trajectory calculations end when the tracks are out of the whole domain (0-40° N, 100-180° E). Fig. 9 shows the simulated frequency of TC occurrence for the El Niño and La Niña years. Comparing with the observed frequency of occurrence in Fig. 3, we can see that the trajectory model can well simulate the primary features of the prevailing TC tracks the El Niño and La Niña years. As shown in Fig. 10, the model can also well simulate the difference of the frequency of TC occurrence between the El Niño and La Niña years.

5. Contributions to changes of the prevailing TC tracks

Chan (1985) suggested that ENSO-related changes in the horizontal and vertical atmospheric circulations cause the formation of an anomalous Walker circulation, which shifts areas of enhanced and suppressed convection, and thus TC formation locations and subsequent track trajectories. Wang and Chan (2002) found that the TC track shift from El Niño years to La Niña years is significantly associated with the changes in the large scale steering flows. Wu and Wang (2004) also suggested that the anomalous large-scale winds associated with different ENSO phases are consistent with different track types. These previous studies pointed out that changes in TC formation locations and large-scale steering flows are responsible for the observed changes in TC prevailing tracks.

TC tracks are simply controlled by two factors: their formation locations and translation vectors. The latter is a combination of large-scale steering and beta drift. As shown in Fig. 2, the interannual changes in translation vectors are dominated by

the changes in large-scale flows. In addition, as we mentioned above, a northwest shift in TC mean formation location from El Niño to La Niña years can be seen in Fig. 5. Further calculation shows that the mean formation location is 15° N, 140° E in the El Niño years and 20° N, 136 ° E in the La Niña years, significantly different at the 95% level. What are the relative contributions of the two factors to the observed changes in TC prevailing tracks?

For this purpose, four numerical experiments are conducted using the trajectory model. As indicated in Table 1, the formation locations and large-scale steering in the El Niño (La Niña) years are used as the first (second) experiment, which is referred to experiment EE (LL). Note that the formation locations used in all four experiments are obtained using the formation model discussed in section 4. In order to demonstrate the influence of formation locations and large-scale steering on the prevailing tracks, two additional experiments, called experiments EL and LE, are performed. In experiment EL (LE), the large-scale steering and formation locations are obtained from El Niño (La Niña) and La Niña (El Niño) years, respectively.

Figure 10 shows the simulated differences of the frequency of TC occurrence between experiments EE and LL. Although the simulated differences in the South China Sea shift northward, the trajectory model can successfully simulate the difference of the frequency of TC occurrence between El Niño and La Niña years. Figures 11a and 11b indicate the influence of the change in the formation locations while the large-scale steering remains unchanged. We can see that the simulated differences of the frequency of TC occurrence between experiments LE and LL (Fig. 11a) and between experiments EE and EL (Fig. 11b) have a similar pattern with positive (negative) anomalies south (north) of 20° N. Figs. 11a and 11b suggest that the change of the formation locations between El Niño and La Niña years contributes

to the enhanced TC activity south of 20° N. The reason is that the TC formation locations shift eastward with a lower mean latitude in the El Niño years than in La Niña years.

Figures 11c and 11d indicate the influence of the change in large-scale steering while the TC formation locations remain unchanged. In experiments EL (EE) and LL (LE), the formation locations are derived from the La Niña (El Niño) years. The simulated differences in the frequency of TC occurrence between experiments EL and LL (Fig. 11c) and between experiments EE and LE (Fig. 11d) also have a similar pattern. As mentioned in section 2, during the El Niño years, TCs that follow prevailing track II tend to move more westward track. Figs. 11c and 11d suggest that the enhanced activity mainly results from the changes in large-scale steering flows. We can see that the change in large-scale steering also leads to increases in the frequency of TC occurrence over north South China Sea and over the ocean to the south of Japan. The latter is largely cancelled by the influence of the changes in formation locations. Therefore the observed changes in the TC prevailing tracks between El Niño and La Niña years are a combined result of the changes in both large-scale steering and formation locations.

6. Summary

Although the interannual variations of TC formation locations and large-scale steering flows are closely associated with TC prevailing tracks, the ENSO influence on TC prevailing tracks in the WNP basin has not well discussed. One of the possible reasons is lack of adequate tools for diagnosing the track change under the ENSO influence. In this study, based on the selected 14 El Niño years and 14 La Niña years during the period 1950-2007, the ENSO influence on TC prevailing tracks is examined with a statistical model for simulating TC formation and a trajectory model

for simulating TC tracks.

Our analysis indicates considerable interannual variations of TC prevailing tracks in the WNP basin. In the El Niño years, although the total number of TC formation in the entire WNP basin does not show significant ENSO influence, the southeast shift of the TC formation location, combined with the changes in large-scale steering flows, leads to the enhanced TC activity south of 20 ºN, in particular east of 130ºE. For TCs that take the northwestward prevailing track (II) affecting East Asia including Taiwan Island, China mainland, Korea and Japan, they tend to move more westward in the El Niño years, but taking a more northward track in the La Niña years. Our simulations with the statistical formation and trajectory models suggest that the prevailing track change is primarily a result of the ENSO-related changes in both large-scale steering flows and TC formation locations.

Acknowledgments. The authors thank Dr. Ho Chang-Hoi and two anonymous reviewers for their valuable suggestions. This research was supported by the typhoon research project (2009CB421503) of the national basic research program (the 973 Program) of China, the National Science Foundation of China (NSFC grant No. 408750387), and the social commonwealth research program of Ministry of Science and Technology of the People's Republic of China (GYHY200806009) and the research project funded by the Colleges and Universities in Jiangsu Province graduate study innovation plan (CX09B_224Z). Weican Zhou is supported by the Jiangsu Key Laboratory of Meteorological Disaster Program (KLME 060206).

References

Camargo, S. J., and A. H. Sobel, 2005: Western North Pacific tropical cyclone intensity and ENSO, *J. Climate*, **18,** 2996-3006.

Camargo, S. J., A. W. Robertson, S. J. Gaffney, P. Smyth, and M. Ghil, 2007: Cluster analysis of typhoon tracks, Part I: Large-scale circulation and ENSO. *J. Climate*, **20,** 3654-3676.

Chan, J. C. L., 1984: An observational study of the physical processes responsible for tropical cyclone motion. *J. Atmos. Sci.*, **41,** 1036-1048

Chan, J. C. L., 1985: Tropical cyclones activity in the northwest Pacific in relation to the El Niño /Southern Oscillation phenomenon. *Mon. Wea. Rev.*, **113**, 599-606.

Chan, J. C. L., 1994: Prediction of the interannual variations of tropical cyclone movement over regions of the western North Pacific. *Int. J. Climatol.*, **14**, 527-538.

Chan, J. C. L., 2000: Tropical cyclones activity over the western North Pacific associated with El Niño and La Niña events. *J. Climate*, **13**, 2960-2972.

Chen, T. C., S. P. Weng, N. Yamazaki, and S. Kiehne, 1998: Interannual variation in the tropical cyclone activity over the western North Pacific, *Mon. Wea. Rev.*, **126**, 1080-1090.

Chia, H. H., and C. F. Ropelewski, 2002: The interannual variability in the genesis location of tropical cyclones in the northwest Pacific, *J. Climate*, **15**, 2934-2944.

Chu, P. S., 2004: ENSO and tropical cyclone activity. Hurricanes and Typhoons: Past, Present, and Potential, R. J. Murnane and K. B. Liu, Eds., Columbia University Press, 297-332.

Dong, K., 1988: El Niño and tropical cyclone frequency in the Australian region and the northwest Pacific. *Aust. Meteor. Mag.*, **36**, 219-225.

Emanuel, K. A., 2005: Increasing destructiveness of tropical cyclones over the past 30 years. *Nature*, **436**, 686-688.

Emanuel, K. A., S. Ravela, E. Vivant, and C. Risi., 2006: A Statistical-Deterministic Approach to Hurricane Risk Assessment. *Bull. Amer. Meteor. Soc.*, **87**, 299–314.

Emanuel, K., R. Sundararajan, and J. Williams, 2008: Hurricanes and global warming: Results from downscaling IPCC AR4 simulations. *Bull. Amer. Meteor. Soc.*, **89**, 347-367.

Fudeyasu, H., S. Iizuka, and T. Matsuura, 2006: Impact of ENSO on landfall characteristics of tropical cyclones over the western North Pacific during the summer monsoon season, *Geophys. Res. Lett.*, **33**, L21815, doi: 10.1029/2006GL0277449.

Goddard, L., and M. Dilley., 2005: El Nino: Catastrophe or opportunity. *J. Climate*, **18**: 651-665.

Gong, D., and C. Ho, 2002: Shift in the summer rainfall over the Yangtze River Valley in the late 1970s. *Geophys. Res. Lett.*, **29(10)**, 1436, doi: 10.1029/2001GL014523.

Hall, T., and Jewson, S., 2007: Statistical modeling of North Atlantic tropical cyclone tracks. *Tellus*, **59(A)**, 486-198.

Ho, C. H., J. J. Baik, J. H. Kim, D.Y. Gong, and C. H. Sui, 2004: Interdecadal changes in summertime typhoon tracks. *J. Climate*, **17**, 1767-1776.

Ho, C. H., J. H. Kim, H. S. Kim, C. H. Sui, and D. Y. Gong, 2005: Possible influence of the Antarctic Oscillation on tropical cyclone activity in the western north Pacific. *J. Geophys. Res.*, **110**, D19104, doi: 10.1029/2005JD005766.

Holland, G. J., 1983: Tropical cyclone motion: Environmental interaction plus a beta effect. *J. Atmos. Sci.*, **40**, 328-342.

Hoyos, C. D., P. A. Agudelo, P. J. Webster, J. A. Curry, 2006: Deconvolution of the Factors Contribution to the Increase in Global Hurricane Intensity. *Science*, **312(5770)**, 94-97.

James, M. K., and Mason, L.B., 2005: Synthetic tropical cyclone database. *J. Wtrwy.*,

Port, Coastal, and Oc. Engrg., **131**, 181-192.

Knutson TR, Tuelya RE, 2004: Impact of CO2-induced warming on simulated hurricane intensity and precipitation: sensitivity to the choice of climate model and convective parameterization. *J. Climate*, **17**, 3477–3495.

Kossin, J. P., K. R. Knapp, D. J. Vimont, R. J. Murnane, and B. A. Harper, 2007: A globally consistent reanalysis of hurricane variability and trends. *Geophys. Res. Lett.*, **34**, L4815, doi: 10.1029/2006GL028836.

Kundzewicz, Z. W., and A. Robson (Eds.), 2000: Detecting trend and other changes in hydrological data[M], *Rep. WCDMP-45, Rep. WMO-TD* **1013**, 157pp., World Meteorol. Org., Geneva, Switzerland.

Lander, M. A., 1994: An exploratory analysis of the relationship between tropical storm formation in the western North Pacific and ENSO. *Mon. Wea. Rev.*, **122**, 636-651.

Li Chongyin, 1985: A study on the influence of El Nino upon typhoon action over Western Pacific. *Acta Meteorologica Sinica*, **45 (2)**, 229-236. (In Chinese)

Li Chongyin, 1986: El Nino and actions of typhoon over the South China Sea. *Journal of Tropical Meteorology*, **2 (2)**, 117-124. (In Chinese)

Li, X., and B. Wang, 1996: Acceleration of hurricane beta drift by shear strain rate of environmental flows. *J. Atmos. Sci.*, **53**, 327-334.

Liu, K. S., and J. C. L. Chan, 2003: Climatological characteristics and seasonal forecasting of tropical cyclones making landfall along the South China Coast. *Mon. Wea. Rev.*, **131**, 1650-1662.

Ren, F., G. Wu, W. Dong, X. Wang, Y. Wang, W. Ai, and W. Li, 2006: Changes in tropical cyclone precipitation over China. *Geophys. Res. Lett.*, **33**, L20702, doi: 10.1029/2006GL027951.

Saunders M., Chandler R., Merchant C, et al., 2000: Atlantic hurricanes and NW Pacific typhoons: ENSO spatial impacts on occurrence and landfall. *Geophys. Res. Lett.*, **27**, 1147-1150.

Smith, R.K., 1991: An analytic theory of tropical cyclone motion in a barotropic shear flow. *Quart. J. Roy. Meteor.*, **117**, 685-714.

Trenberth, K. E., 1997: The definition of El Niño. *Bull. Amer. Meteor. Soc.*, **78**, 2771–2777.

Trenberth, K. E., 2005: Uncertainty in Hurricanes and Global Warming. *Science.*, **308(5729)**, 1753-1754.

Tu, J. Y., C. Chou, and P. S. Chu, 2009: The abrupt shift of typhoon activity in the vicinity of Taiwan and its association with western North Pacific-East Asian climate change, *J. Climate*, **22**, 3617-3628.

Ulrich, W., and R. K. Smith, 1991: A numerical study of tropical cyclone motion using a barotropic model, II: motion in spatially-varying large-scale flow. *Quart. J. Roy. Meteor. Soc.*, **117**, 107-124.

Wang, B., and X. Li, 1995: Propagation of a tropical cyclone in meridionally-varying zonal flows: An energetics analysis. *J. Atmos. Sci.*, **52**, 1421-1433.

Wang, B., X. Li, and L. Wu, 1997: Direction of hurricane beta drift in horizontally sheared flows. *J. Atmos. Sci.*, **54**, 1462-1471.

Wang, B., and J. C. Chan, 2002: How strong ENSO events affect tropical storm activity over the western North Pacific. *J. Climate*, **13**, 1517-1536.

Webster, P. J., G. J. Holland, J. A. Curry, and H. R. Chang, 2005: Changes in tropical cyclone number, duration, and intensity in a warming environment. *Science*, **309**, 1844-1846.

Williams, R. T., and J. C. L. Chan, 1994: Numerical studies of the beta effect in

tropical cyclone motion, Part II: Zonal mean flow. *J. Atmos. Sci.*, **51**, 1065-1076.

Wu, G.., and N. C. Lau, 1992: A GCM simulation of the relationship between tropical storm formation and ENSO. *Mon. Wea. Rev.*, **120**, 958-977.

Wu, L., and B. Wang, 2004: Assessing impacts of global warming on tropical cyclone tracks. *J. Climate*, **17**, 1686-1698.

Wu, L., and B. Wang, 2008: What has changed the proposition of intense hurricanes in the last 30 years? *J. Climate*, **21**, 1432-1439.

Wu, L., B. Wang, and S. A. Braun, 2008: Implications of tropical cyclone power dissipation index. *Int. J. Climatol.*, **28**, 727-731.

Wu, L., B. Wang, and S. Geng, 2005: Growing typhoon influence on east Asia. *Geophys. Res. Lett.*, **32**, L18703, doi: 10.1029/2005GL022937.

Wu, M. C., W. L. Chang, and W. M. Leung, 2004: Impacts of El Nino Southern Oscillation events on TC landfalling activity in the western North Pacific. *J. Climate*, **17**, 1419-1428.

Yoo, S.-H., C.-H. Ho, S.Yang, H.-J. Choi, and J.-G. Jhun, 2004: Influence of tropical-western and extratropical Pacific sea surface temperatures on the east and Southeast Asian climate in the summers of 1993-94. *J.Climate,* **17**, 2673-2687.

Zhao, H., L. Wu, and W. Zhou, 2009: Observational Relationship of Climatologic Beta Drift with Large-Scale Environmental Flows. *Geophys. Res. Lett.,* **36,** L18809, doi: 10.1029/2009GL040126.

Table Captions

Table 1 Experiments for simulating the TC tracks by using the approach proposed in this study. The first column represents the name of experiments, the second the mean large-scale steering for El Niño (La Niña) years and the third the simulation of genesis points based on the observed of El Niño (La Niña) years.

Figure Captions

Figure 1 Niño-3.4 SSTA index averaged over July to September (JAS) according to the percentile method proposed by Camargo et al. (2007). The selected warm (cool) years are shown in red (blue) with black bars for neutral years.

Figure 2 The difference of climatological tropical cyclone translation vectors (a) and the climatological layer (850-300hpa) mean large-scale steering flows (b) between the El Niño years and La Niña years in TC peak season (Jul-Sep). Contour intervals are 0.2 ms^{-1}.

Figure 3 The observed frequency of TC occurrence at 2.5° *2.5° resolution in the TC peak season (Jul-Sep) derived from the JTWC best-track data for (a) El Niño and (b) La Niña years with contour intervals of 3.0.

Figure 4 Observed differences of the frequency of TC occurrence in the TC peak season (Jul-Sep) between El Niño and La Niña years. The change with the shading is statistically significant at the 95% level.

Figure 5 The frequency of TC formation at 2.5° *2.5° resolution in the TC peak season (Jul-Sep) derived from the JTWC best-track data for (a) El Niño and (b) La Niña years with intervals of 0.3. Cross dots are the observed TC formation positions.

Figure 6 the out-of sample log-likehood (y-axis) versus bandwidths (x-axis) for kernel density function described in expression (2) and the optimal bandwidths are selected for (a) El Niño and (b) La Niña years using the Cross-validation

method based on the observed information over TC peak seasons (Jul-Sep).

Figure 7 Kernel formation PDF with bandwidth 5° (top left), 2.9° (top right), and 1.5° (down) for El Niño years The PDFs are normalized to the unit maximum.

Figure 8 the simulated frequency of TC formations in the TC peak season (Jul-Sep) for (a) El Niño and (b) La Niña years with contour intervals of 0.2. The cross dots are the simulated TC formation positions.

Figure 9 The simulated frequency of TC occurrence at 2.5° *2.5° resolution in the TC peak season (Jul-Sep) for (a) El Niño and (b) La Niña years with contour intervals of 3.0.

Figure 10 Simulated differences of the frequency of TC occurrence in the TC peak season (Jul-Sep) between El Niño and La Niña years, which are calculated as the difference of the frequency of TC occurrence between EE (El Niño steering and El Niño formation locations) and LL (La Niña steering and La Niña formation locations).

Figure 11 Simulated differences of the frequency of TC occurrence in the TC peak season (Jul-Sep) between (a) LE(La Niña steering and El Niño formation locations) and LL(La Niña steering and La Niña formation locations), (b) EE(El Niño steering and El Niño formation locations) and EL(El Niño steering and La Niña formation locations), (c) EL and LL, and (d) EE and LE,, indicating the influences of changes in formation locations (a and b) and large-scale flows (c and d).

Table 1 Experiments for simulating the TC tracks by using the approach proposed in this study. The first column represents the name of experiments, the second the mean large-scale steering for El Niño (La Niña) years and the third the simulation of genesis points based on the observed of El Niño (La Niña) years.

Experiments	Large-scale steering	Formation locations
EE	El Niño	El Niño
LL	La Niña	La Niña
EL	El Niño	La Niña
LE	La Niña	El Niño

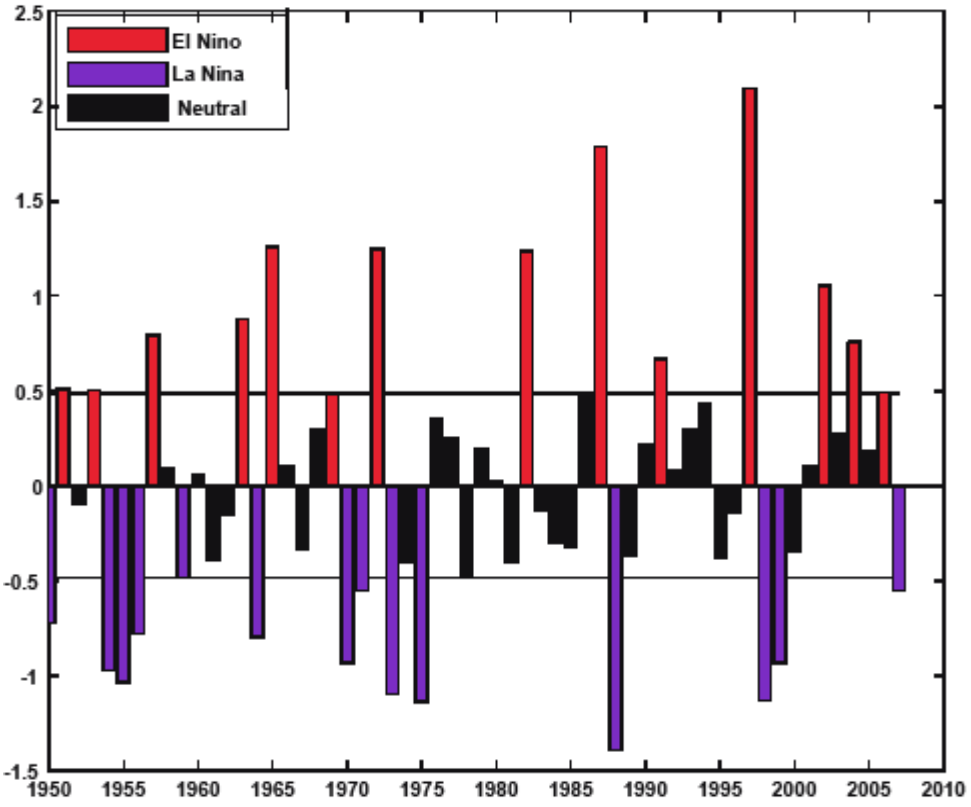

Figure 1 Niño-3.4 SSTA index averaged over July to September (JAS) according to the percentile method proposed by Camargo et al. (2007). The selected warm (cool) years are shown in red (blue) with black bars for neutral years.

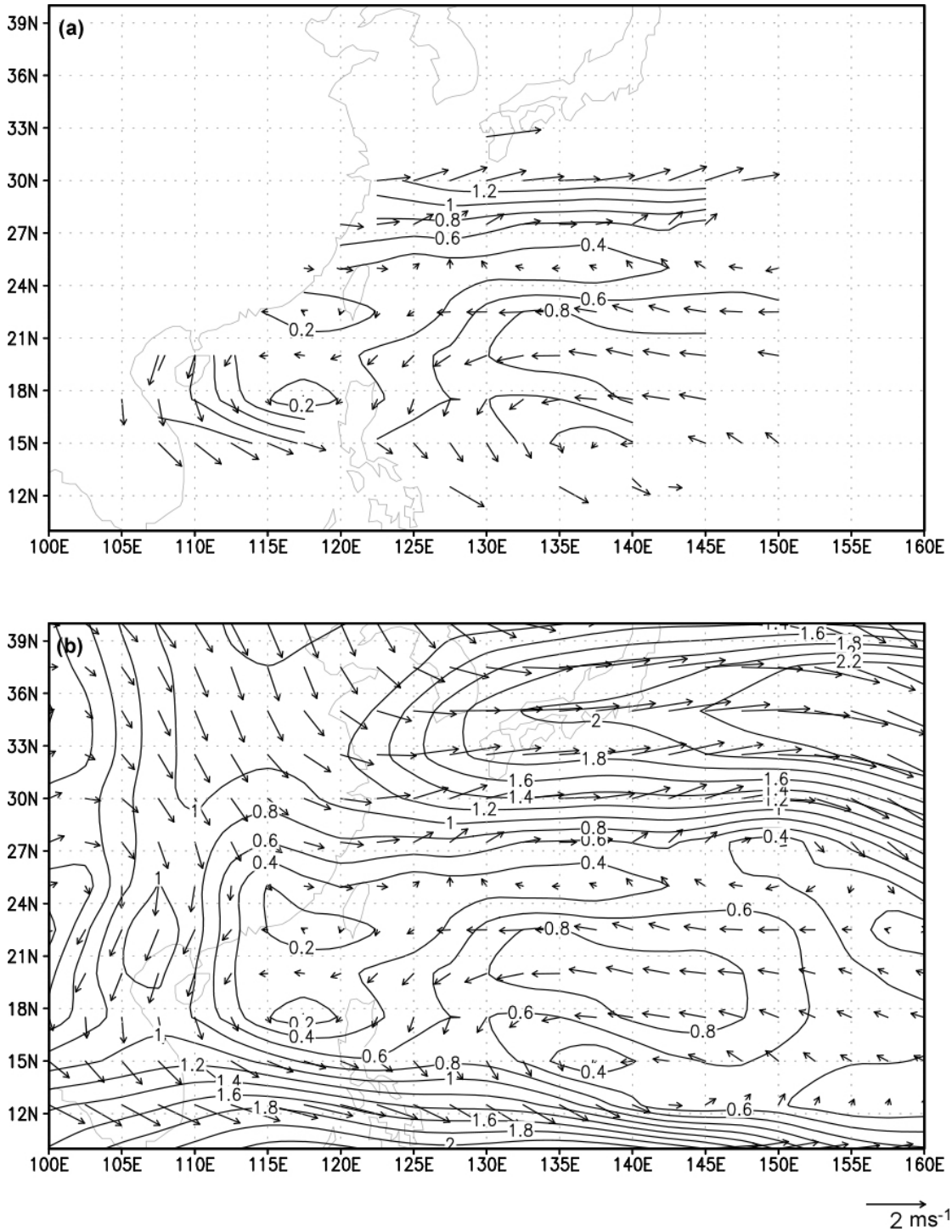

Figure 2 The difference of climatological tropical cyclone translation vectors (a) and the climatological layer (850-300hpa) mean large-scale steering flows (b) between the El Niño years and La Niña years in TC peak season (Jul-Sep). Contour intervals are 0.2 ms^{-1}.

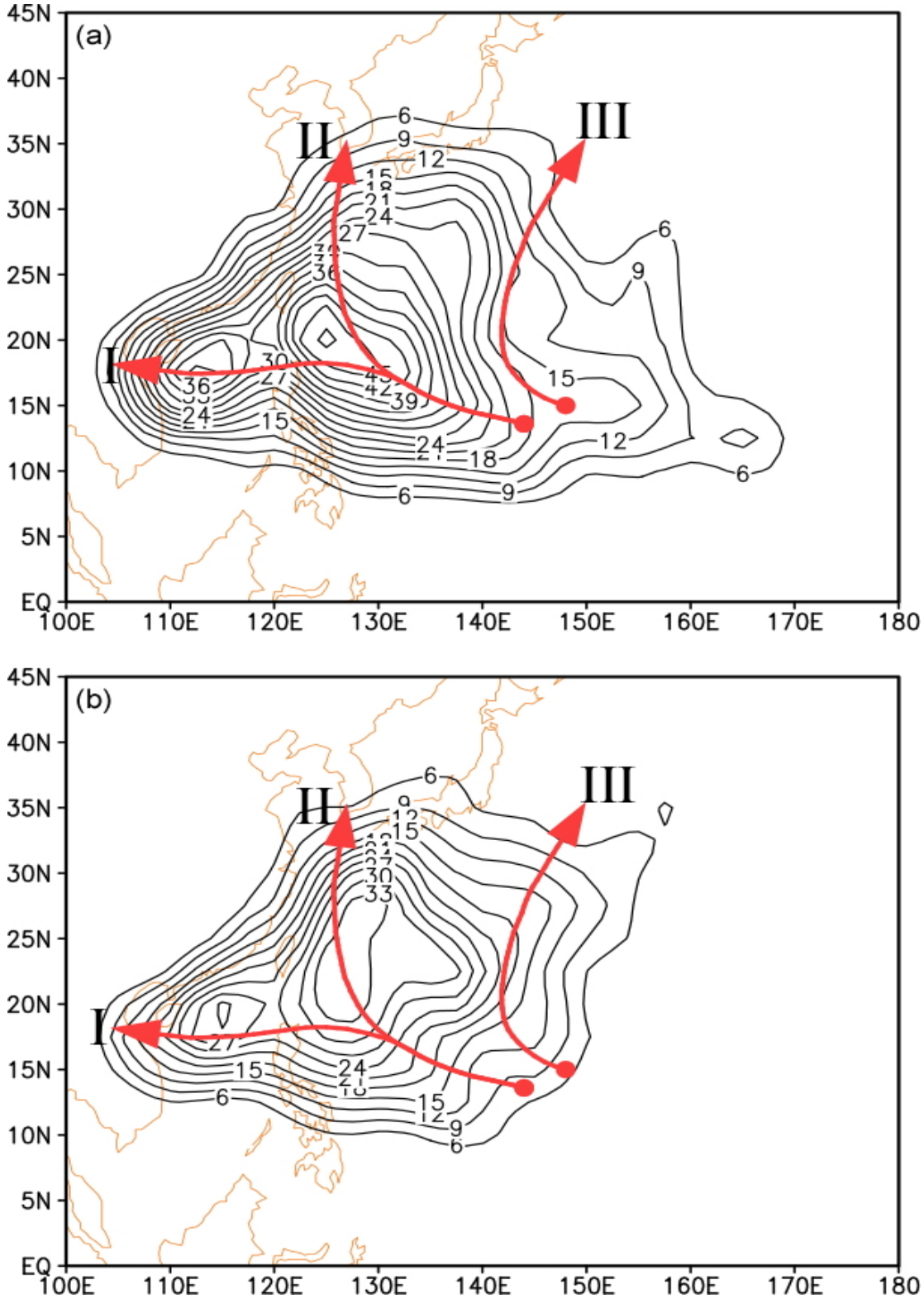

Figure 3 The observed frequency of TC occurrence at 2.5° *2.5° resolution in the TC peak season (Jul-Sep) derived from the JTWC best-track data for (a) El Niño and (b) La Niña years with contour intervals of 3.0.

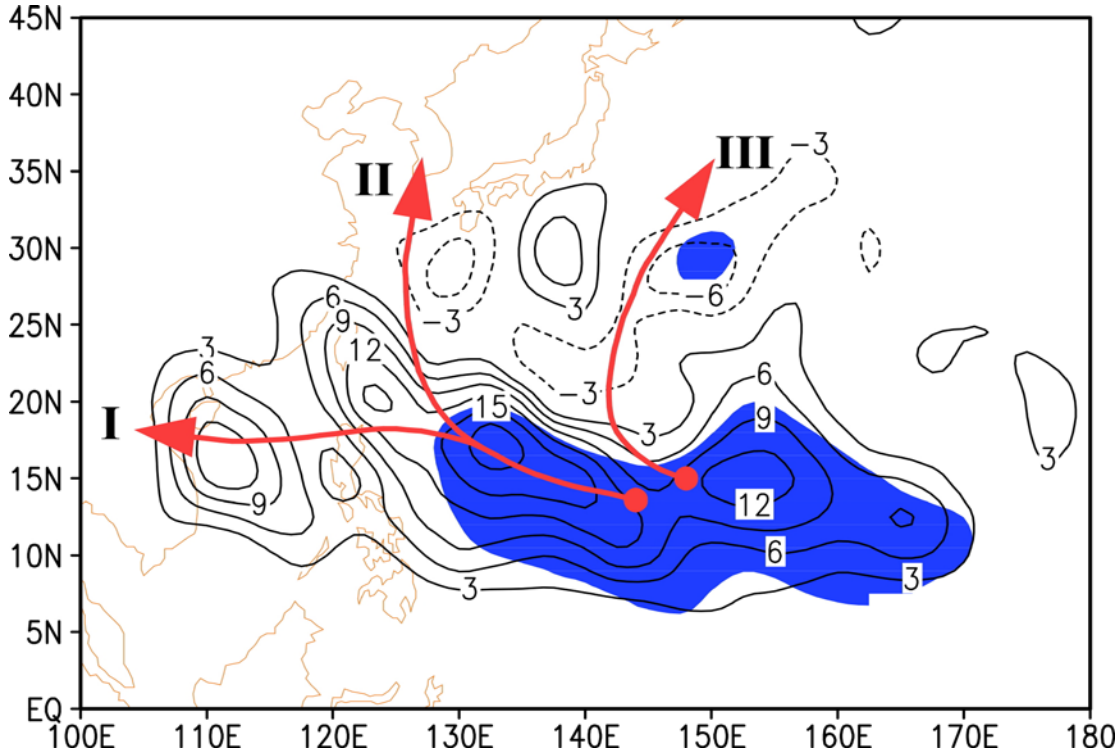

Figure 4 Observed differences of the frequency of TC occurrence in the TC peak season (Jul-Sep) between El Niño and La Niña years. The change with the shading is statistically significant at the 95% level.

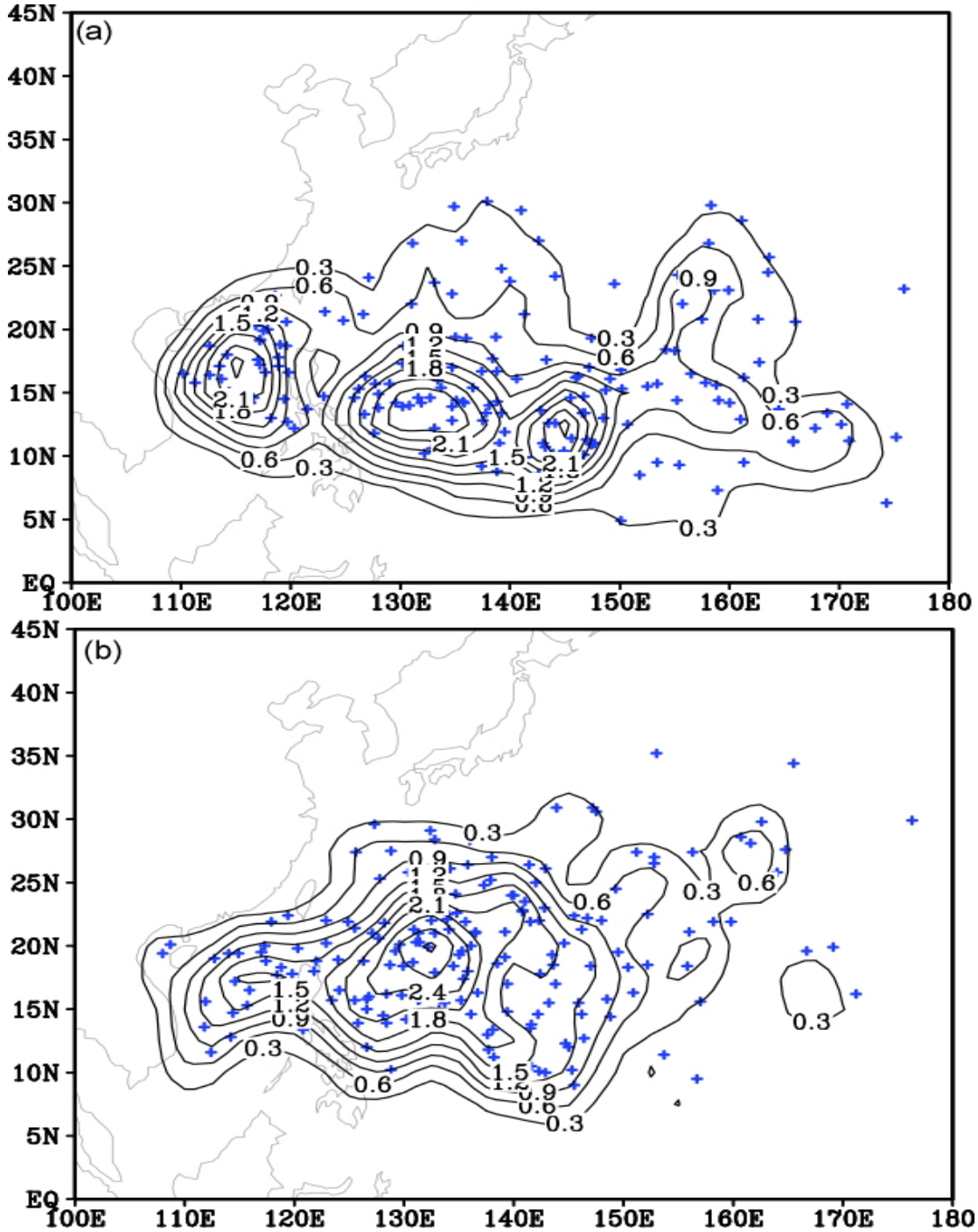

Figure 5 The frequency of TC formation at 2.5° *2.5° resolution in the TC peak season (Jul-Sep) derived from the JTWC best-track data for (a) El Niño and (b) La Niña years with intervals of 0.3. Cross dots are the observed TC formation positions.

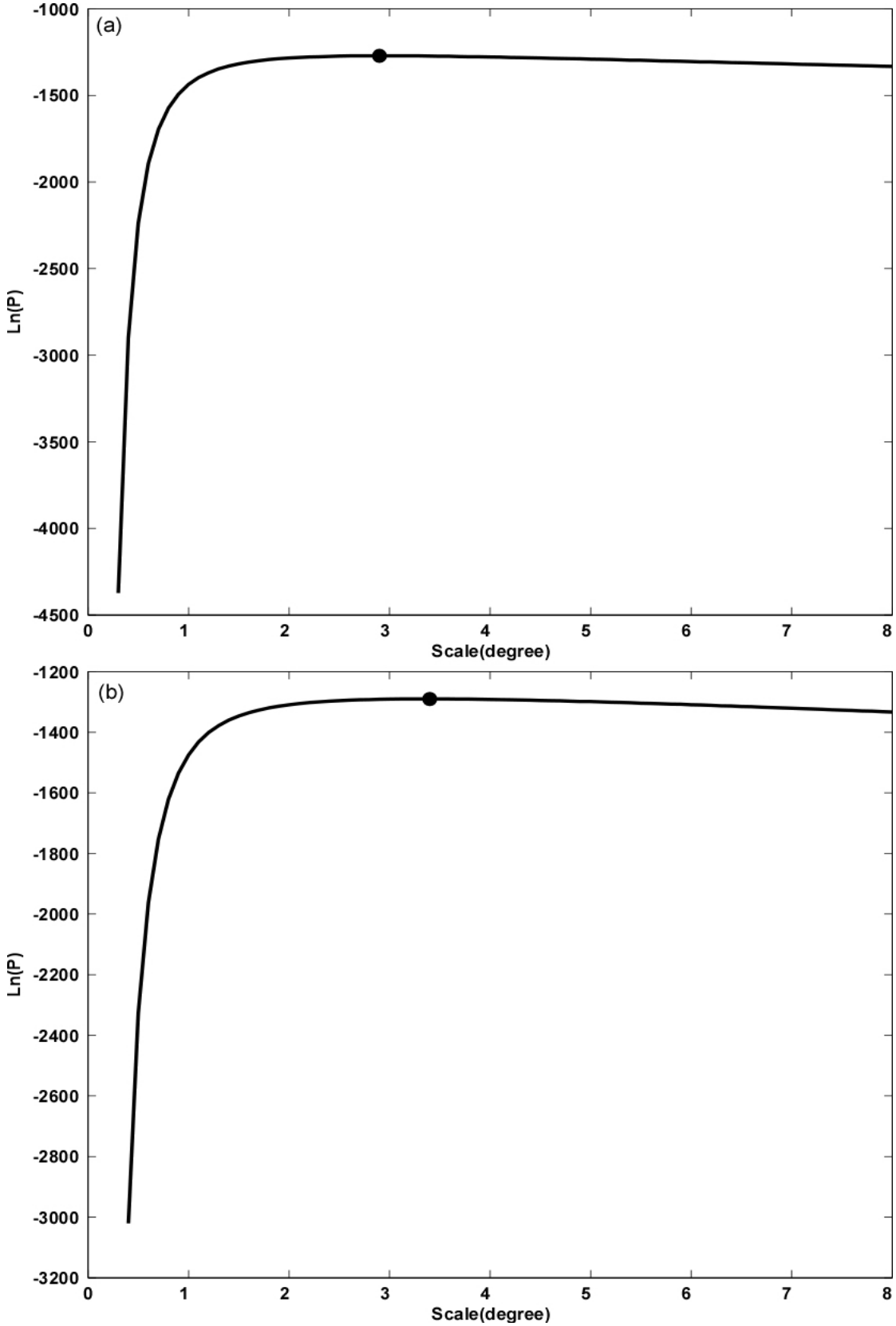

Figure 6 the out-of sample log-likehood (y-axis) versus bandwidths (x-axis) for kernel density function described in expression (2) and the optimal bandwidths are selected for (a) El Niño and (b) La Niña years using the Cross-validation method based on the observed information over TC peak seasons (Jul-Sep).

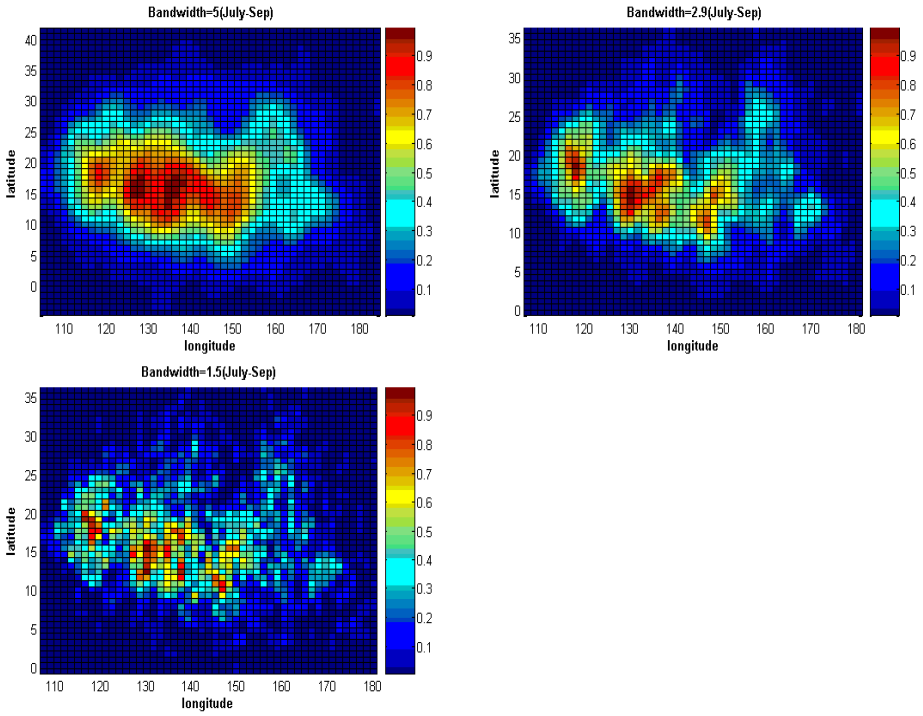

Figure 7 Kernel formation PDF with bandwidth 5° (top left), 2.9° (top right), and 1.5° (down) for El Niño years The PDFs are normalized to the unit maximum.

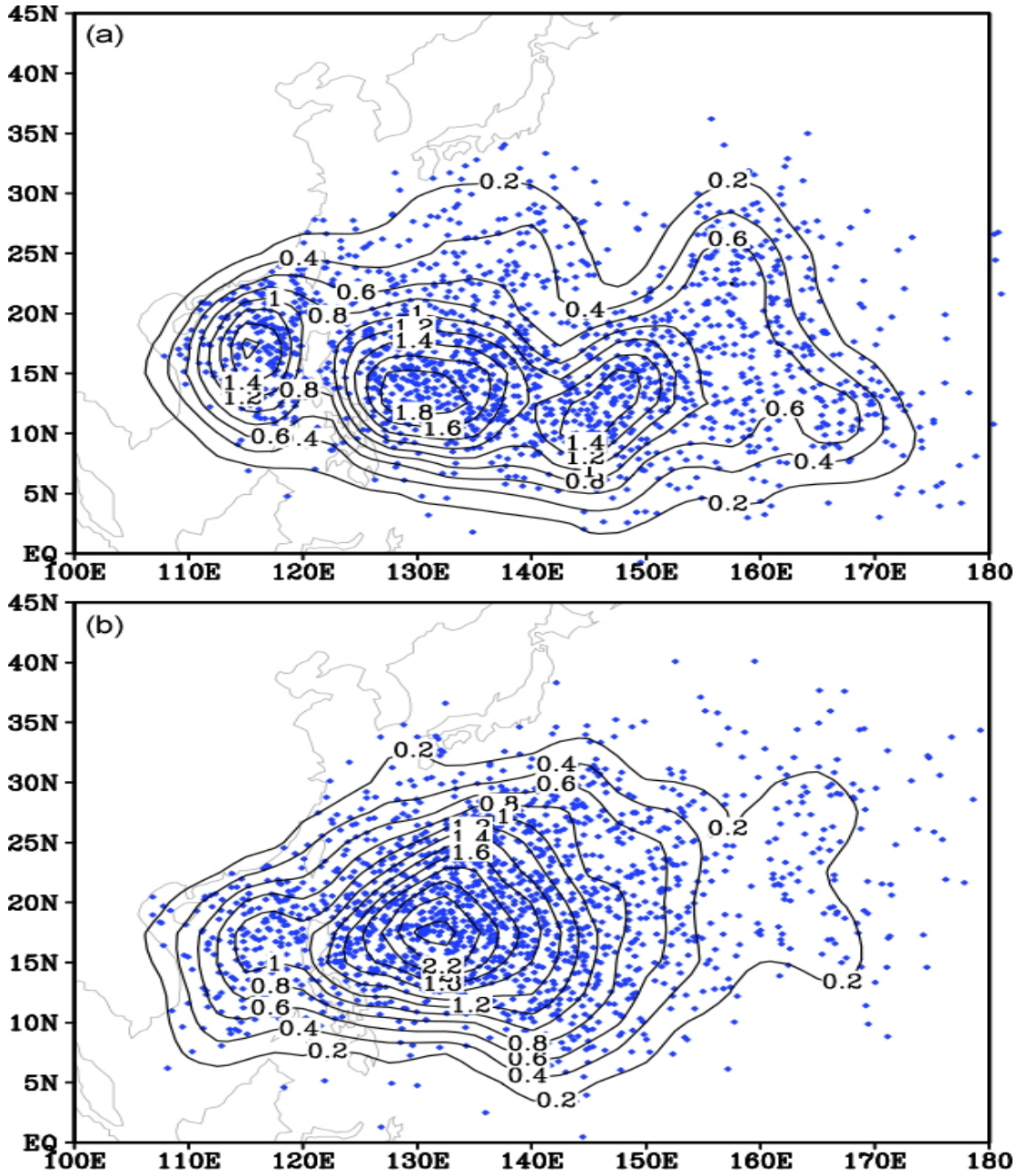

Figure 8 the simulated frequency of TC formations in the TC peak season (Jul-Sep) for (a) El Niño and (b) La Niña years with contour intervals of 0.2. The cross dots are the simulated TC formation positions.

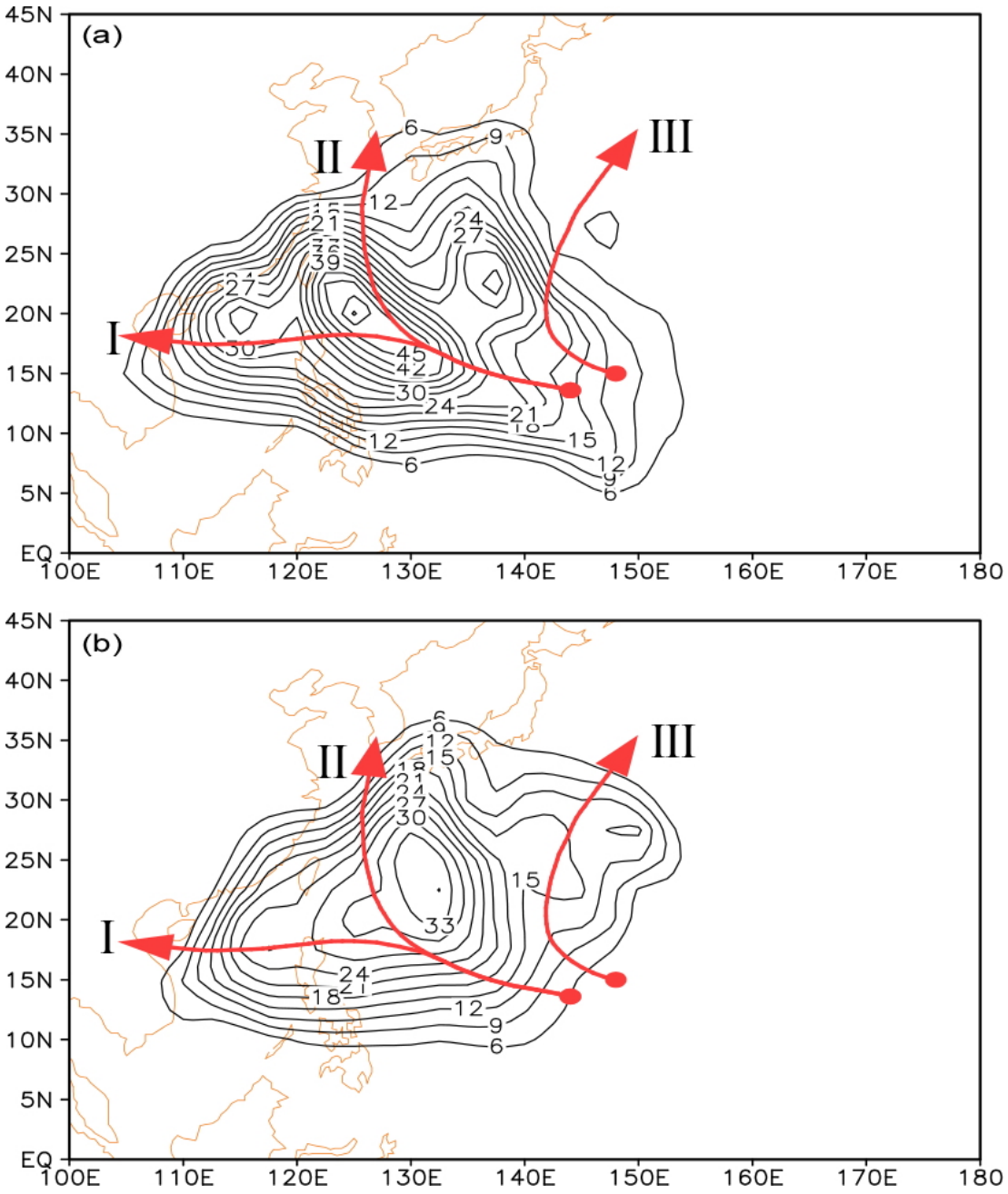

Figure 9 The simulated frequency of TC occurrence at 2.5° *2.5° resolution in the TC peak season (Jul-Sep) for (a) El Niño and (b) La Niña years with contour intervals of 3.0.

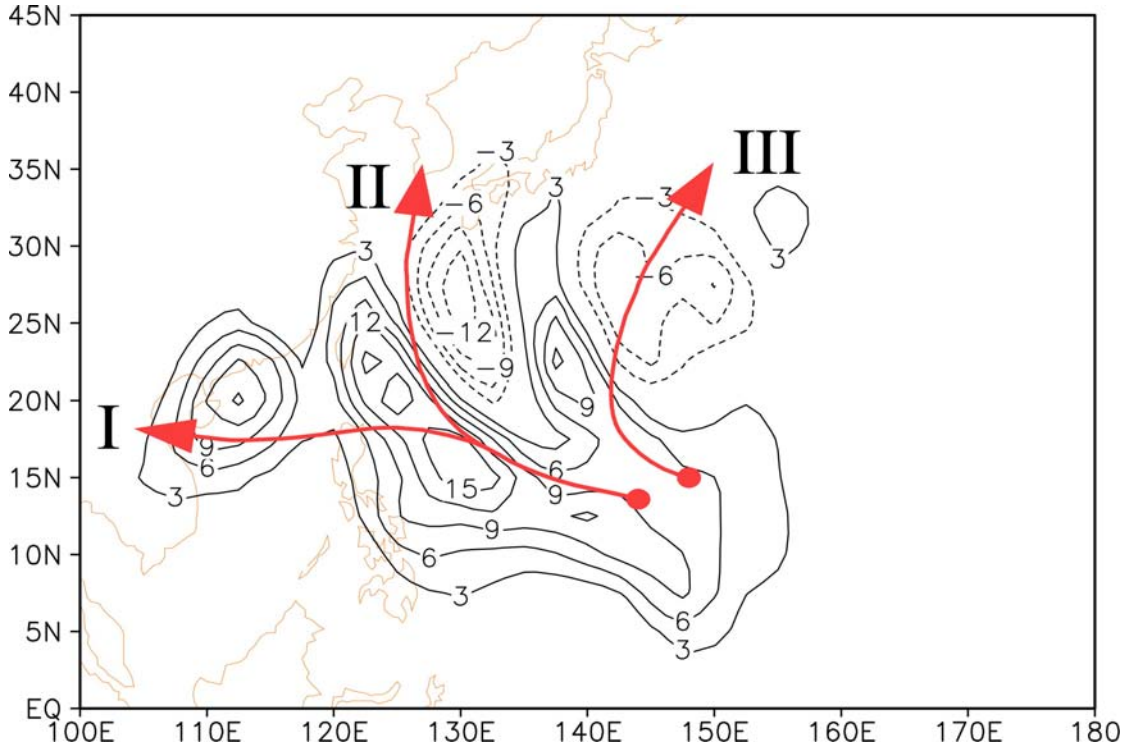

Figure 10 Simulated differences of the frequency of TC occurrence in the TC peak season (Jul-Sep) between El Niño and La Niña years, which are calculated as the difference of the frequency of TC occurrence between EE (El Niño steering and El Niño formation locations) and LL (La Niña steering and La Niña formation locations).

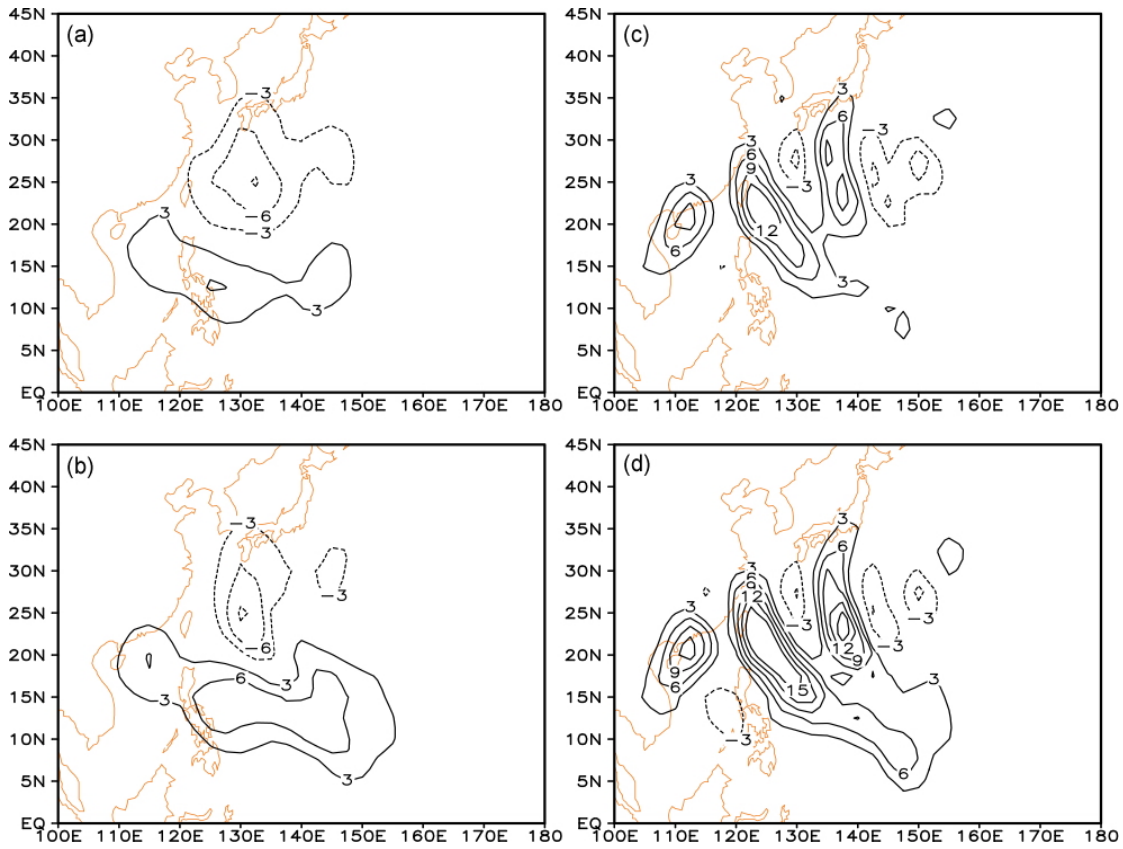

Figure 11 Simulated differences of the frequency of TC occurrence in the TC peak season (Jul-Sep) between (a) LE(La Niña steering and El Niño formation locations) and LL(La Niña steering and La Niña formation locations), (b) EE(El Niño steering and El Niño formation locations) and EL(El Niño steering and La Niña formation locations), (c) EL and LL, and (d) EE and LE,, indicating the influences of changes in formation locations (a and b) and large-scale flows (c and d).